

Convex optimization for non-equilibrium steady states on a hybrid quantum processor

Jonathan Wei Zhong Lau,^{1,*} Kian Hwee Lim,^{1,*} Kishor
Bharti,^{2,3} Leong-Chuan Kwek,^{1,4,5,6} and Sai Vinjanampathy^{1,7,8}

¹Centre for Quantum Technologies, National University of Singapore, 3 Science Drive 2, Singapore 117543

²Joint Center for Quantum Information and Computer Science and Joint Quantum Institute,
NIST/University of Maryland, College Park, Maryland 20742, USA

³Institute of High Performance Computing (IHPC),
Agency for Science Technology and Research (A*STAR), 1 Fusionopolis Way,
#16-16 Connexis, Singapore 138632, Republic of Singapore

⁴MajuLab, CNRS-UNS-NUS-NTU International Joint Research Unit, UMI 3654, Singapore

⁵National Institute of Education, Nanyang Technological University, 1 Nanyang Walk, Singapore 637616

⁶School of Electrical and Electronic Engineering Block S2.1, 50 Nanyang Avenue, Singapore 639798

⁷Department of Physics, Indian Institute of Technology-Bombay, Powai, Mumbai 400076, India[†]

⁸Centre of Excellence in Quantum Information, Computation, Science and Technology,
Indian Institute of Technology Bombay, Powai, Mumbai 400076, India.

Finding the transient and steady state properties of open quantum systems is a central problem in various fields of quantum technologies. Here, we present a quantum-assisted algorithm to determine the steady states of open system dynamics. By reformulating the problem of finding the fixed point of Lindblad dynamics as a feasibility semidefinite program, we bypass several well known issues with variational quantum approaches to solving for steady states. We demonstrate that our hybrid approach allows us to estimate the steady states of higher dimensional open quantum systems and discuss how our method can find multiple steady states for systems with symmetries.

Introduction.— Understanding open system evolution is central to modern quantum technologies such as computing, thermodynamics [1–3], chemistry [4], and quantum transport [5]. Since such evolution maps initial quantum states to future states, both transient and steady state properties are available in the structure of the evolution operator. Sparing few analytically tractable systems, generic open system evolution has to be solved numerically to understand both transient and steady state dynamics of the system. Such classical simulation techniques are limited due to the exponential growth of Hilbert space. Some specific sampling problems can be simulated classically [6–9] and tensor networks can be deployed for scenarios with limited entanglement growth [10–17]. For generic open system evolution by contrast, such a classical simulation is limited to few dozen qubits in the presence of symmetries. Usually, such problems are either simplified by the presence of strong local dissipators which reduce the amount of entanglement generated or by low dimensionality of the problem. Outside of these special cases, the issue of generic open system evolution has remained unsolved.

The advent of small quantum computers heralds a new variety of solutions to the problem of determining the transient and steady state solutions to such open system evolution. One strategy involves implementing open system evolution on an intermediate scale quantum computer and tomographically measuring the quantum state at various times [18]. An equivalent method for completely positive maps would be to quantum simulate and measure the Choi matrix associated with the open system evolution [19–21]. These tomographic methods require exponentially large number of measurements and

hence are practically infeasible. Another group of closely-related strategies involves first implementing \mathcal{L} , the Liouville superoperator associated with the open system evolution, on a quantum computer. After implementing \mathcal{L} on a quantum computer, the different strategies to find the non equilibrium steady states (NESS) include methods like a combination of Trotterisation and imaginary time evolution using \mathcal{L} [22], quantum phase estimation on \mathcal{L} [23], and variational quantum algorithms (VQAs) to find the kernel of $\mathcal{L}^\dagger \mathcal{L}$ [24]. These different but related strategies have their own individual drawbacks. Trotterisation and phase estimation approaches are known to be infeasible on our current quantum devices with short coherence times, and the variational optimisation approaches suffers from the difficulty of optimising over a non-convex space [25–27]. Lastly, all of these methods that rely on the superoperator representation \mathcal{L} of the open system evolution suffer from the large dimensionality of the Liouville space.

In this paper, we propose a hybrid algorithm for the determination of NESS. Through our approach, the steady state problem can be recast as solving a feasibility semidefinite program (SDP) [28–30]. We show that such an approach to find the NESS is viable on a NISQ device. Our first contribution is to restate the NESS problem as a feasibility SDP, which is an SDP where the goal is to find a feasible solution satisfying the positive semidefinite and linear constraints [28–30]. Our second contribution is that we do not use a variational quantum state/circuit as the ansatz [24, 31–33]. By doing so, we bypass the problems [34–37] associated with training variational quantum algorithms with their non-convex landscape, which is known to be non-deterministic polynomial-time (NP)

hard [25–27]. We show that our algorithm naturally enforces positivity constraint of a physical density matrix and provides methods to enforce additional constraints systematically while retaining the advantages of quantum-assisted methods [35, 37–40], like providing a method to systematically gain a more expressible, problem aware ansatz.

Non-equilibrium steady states.— Open system dynamics under Born, Markov and secular approximations are often described by a time-local master equation given by $\dot{\rho} = L[\rho]$ where

$$L[\rho] = -i[H, \rho] + \sum_n \gamma_n \left(A_n \rho A_n^\dagger - \frac{1}{2} \{A_n^\dagger A_n, \rho\} \right).$$

Such an evolution preserves conditions for valid density matrices. The transient and steady states of this evolution are characterized by the spectrum of the Liouville superoperator [5], defined by the vectorization $B\rho C \rightarrow C^* \otimes B|\rho\rangle$. Steady states are understood to satisfy $L[\rho] = 0$ or equivalently $\mathcal{L}|\rho\rangle = 0$, where \mathcal{L} is the Liouville superoperator that arises from the vectorisation of L . Since these steady states do not usually correspond to a thermal equilibrium, they are referred to as non-equilibrium steady states (NESS). We refer to the problem of obtaining the steady state(s) of a given Liouville evolution as the NESS problem, which is solved classically by matrix diagonalization. However, due to the increase in dimensionality, diagonalization of the full spectrum is usually unfeasible. Furthermore, the evolution of n -dimensional density matrices in Liouville space are represented by $n^2 \times n^2$ matrices. This squared dimensionality implies that numerical techniques can find the entire spectrum of only modest open quantum systems, usually relying on Arnoldi type methods [41–44], which become quite cumbersome for many-body systems of moderate size.

Hence, there is interest in understanding if quantum computers, with their inherent dimensionality advantages in simulating quantum systems over classical computers, can solve the NESS problem. For NISQ devices, it was shown that the NESS problem can be mapped to a variational problem in Liouville space [24]. The subsequent variational problem is solved by using a parameterized quantum state or quantum circuit as the ansatz, and relies on forms of VQA. This approach has two main concerns. Firstly, it is unclear how to systematically enforce the positivity constraint for the density matrix in this approach, as the variational quantum state/quantum circuit, which is a vector, must eventually correspond to a physical density matrix using the vectorisation described above. Secondly, optimizing over the set of pure states tends to not be convex and hence difficult, and indeed has been shown to be NP-hard, reasons including the parameter landscape containing exponentially many persistent local minima that are far from the global minimum [25–27] (See Supplemental Material [45]). Other

VQA methods that do not explicitly rely on this map to Liouville space [31] face similar problems.

Quantum Feasibility SDP Approach.— We circumvent the non-convex optimization problem in the Liouville space by optimizing over the convex set of density matrices. This allows us to directly apply a feasibility SDP, one consequence of which is that we can now systematically enforce the positive semidefinite condition. A feasibility SDP admits the following form: Find X , $X \in \mathcal{S}_+^l$, such that $\text{Tr}(C_k X) = v_k, \forall k \in \{1, 2, \dots, c\}$. Here, \mathcal{S}_+^l represents the set of $l \times l$ symmetric PSD matrices. This is the problem of determining if it is possible to find a matrix X subject to the PSD constraint and the other given constraints. The matrices C_k belong to the set of symmetric matrices \mathcal{S}^l for $k \in \{1, 2, \dots, c\}$. The k -th element of vector $v \in \mathbb{R}^c$ is denoted by v_k . SDPs can be formulated for complex-valued matrices via a cone of Hermitian positive semidefinite matrices i.e. $X \in \mathcal{H}_+^l$. Since SDPs for real valued matrices are a special case of SDPs for complex-valued matrices, we will consider the latter case in this paper. Since $\dot{\rho} = L[\rho]$ is linear in ρ , the NESS problem is a feasibility SDP.

We consider a state ansatz of the form

$$\rho = \sum_{i,j} \beta_{ij} |\chi_i\rangle \langle \chi_j|. \quad (1)$$

Here, β_{ij} are matrix elements of a positive semidefinite matrix β , whereas $|\chi_i\rangle$ states can be from any set of quantum states. We see that β being positive semidefinite is both a necessary and sufficient condition for ρ to be positive semidefinite. The condition $\text{Tr}(\rho) = 1$ becomes $\text{Tr}(\beta E) = 1$, where E is a matrix with matrix elements $E_{ij} = \langle \chi_i | \chi_j \rangle$.

With the chosen ansatz, the NESS problem becomes

$$\text{Find } \beta \text{ s.t. } -i(D\beta E - E\beta D) + \sum_n \gamma_n \left(R_n \beta R_n^\dagger - \frac{1}{2} F_n \beta E - \frac{1}{2} E \beta F_n \right) = 0, \quad (2)$$

$$\beta \succcurlyeq 0, \quad (3)$$

$$\text{Tr}(\beta E) = 1, \quad (4)$$

where γ_n are the strengths of the dissipators, D, R, F are matrices defined as $D_{ij} = \langle \chi_i | H | \chi_j \rangle$, $(R_n)_{ij} = \langle \chi_i | A_n | \chi_j \rangle$ and $(F_n)_{ij} = \langle \chi_i | A_n^\dagger A_n | \chi_j \rangle$. This reduction of the NESS problem to a feasibility SDP [29, 78] defined over β is motivated by the idea that a judicious choice of the states $|\chi_i\rangle$ in some problem-aware manner could possibly allow us to do an optimisation over a smaller dimensional convex landscape (compared to ρ). Furthermore, the positive semidefiniteness condition of ρ can be enforced naturally. We utilize CVX [79], that relies on a disciplined convex programming algorithm [80, 81].

We can also easily enforce additional linear constraints of the form $\text{Tr}(\beta X) = x$, where X and x are arbitrary matrices and values respectively. This feature of our scheme

is absent in the existing algorithms for solving NESS on NISQ devices and is further discussed below.

The overlap values for the matrix elements of the E, D, R, F matrices can be measured on a NISQ quantum computer [48]. In general, how we choose the $|\chi_i\rangle$ states to form our ansatz will contribute strongly to how our algorithm scales. For a general Hamiltonian, absent of exploitable symmetries, the size of the optimal ansatz will grow exponentially with the size of the problem. (see Supplemental Information [45]). Even in the worst case where we require exponentially large numbers of $|\chi_i\rangle$ states in our ansatz, we do not map the problem to an equivalent one in Liouville space and avoid the aforementioned squared dimensionality that comes from doing optimization in Liouville space. Hence in the worst case, our method is at least quadratically better than analogous variational algorithms.

Unless otherwise stated, we choose cumulative \mathcal{K} moment states ($\mathbb{C}\mathcal{S}_K$ states) [39] which provide us with a systematic way to generate an increasingly expressible problem aware ansatz. These states rely heavily on calculating expectation values of powers of the Hamiltonian $\langle \psi | H^k | \psi \rangle$ which can be done efficiently [53, 54]. They alternatively can also be easily obtained by calculating the expectation value of Pauli strings [38, 39] (see [45] for details). By using the $\mathbb{C}\mathcal{S}_K$ states as an ansatz, the size of the β matrix that will be calculated scales as δ^K , where δ is the number of terms in the Hamiltonian, for small K . While this is typically not scalable, we emphasize that our method need not use $\mathbb{C}\mathcal{S}_K$ states as its ansatz. Our main contribution is in approaching the steady state problem in terms of a SDP, and the choice of ansatz in our paper is secondary. A more efficient method of generating an ansatz can be used, if we have greater knowledge of the underlying symmetries of the system. Note that the SDP itself could also be sped up with the help of a quantum computer [82].

The algorithm can hence be summarised as (a) choose a hybrid ansatz for ρ using a set of chosen quantum states $\{|\chi_i\rangle\}$ (b) calculate the entries of the overlap matrices on the quantum computer, (c) we use the matrices in a SDP optimization routine run on a classical computer to obtain the approximate NESS.

Examples.— We demonstrate our algorithm with some examples. Consider a two qubit transverse field Ising model with the Hamiltonian $H_2 = (1/2)\sigma_Z^1\sigma_Z^2 + g\sigma_X^1 + g\sigma_X^2$, together with local dissipators $A_1 = \sigma_Z^1$, $A_2 = (1/2)(\sigma_X^1 - i\sigma_Y^1)$, $A_3 = \sigma_Z^2$ and $A_4 = (1/2)(\sigma_X^2 - i\sigma_Y^2)$. For all instances presented in Fig. 1, our hybrid algorithm outputs a density matrix ρ that is unit trace, Hermitian, positive semidefinite and that fulfils the NESS condition $\dot{\rho} = 0$. To study the robustness of the algorithm for larger chains, in Fig. 2 we show simulation results for the transverse field Ising model up to eight qubits. For the five qubit and eight qubit systems presented in Fig. 2, when increasing K , we choose from the $\mathbb{C}\mathcal{S}_K$ ansatz, a

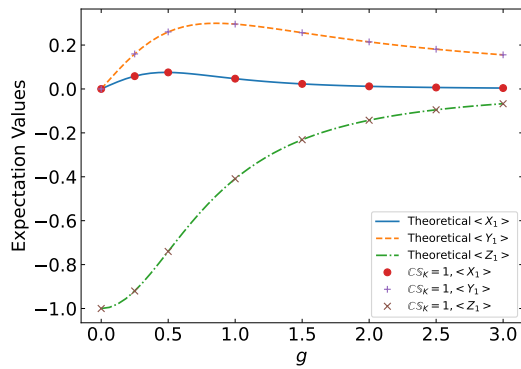


FIG. 1. Expectation values for two qubit transverse field Ising model. γ_S set at 1. Fidelity is equal to 1 for all values of g . Our method gives strong agreement with the theoretical results.

random subset of new states, as highlighted in the Supplementary Information. A comparison with the existing NISQ approach in [24] for the eight qubit case is also given in the Supplementary Information [45].

We note that for the model chosen, as g increases, the exact NESS solution has larger rank and is less sparse. We find that for such situations, a larger ansatz size is needed to obtain an approximate NESS with similar fidelity. We also note that the $\mathbb{C}\mathcal{S}_K$ ansatz performs efficiently when the steady states are low rank. When this is not the case, it is expected that any NISQ algorithm based on such ansatzes will underperform. Likewise, we note that another choice that significantly influences the ansatz is the choice of initial states, where recent results on solving the ground state problem can aid in providing useful initial states [83].

Strong symmetries.— One additional complication with the NESS problem is that systems with symmetries can exhibit multiple NESS [5]. Our algorithm can also be extended to certain cases where multiple NESSs are expected. If there is a strong symmetry in the system, then the Hilbert space can be decomposed into the symmetry subspaces, namely

$$\mathcal{H} = \bigoplus_{\alpha=1}^{n_U} \mathcal{H}_\alpha, \quad \mathcal{H}_\alpha = \text{Span} \left\{ |\psi_\alpha^{(k)}\rangle \right\}, k \in [1, d_\alpha]. \quad (5)$$

Here $|\psi_\alpha^{(k)}\rangle$ are the eigenvectors of the unitary U which characterise the system's strong symmetry. The corresponding eigenvalues are u_α , $\alpha \in [1, n_U]$, where $1 \leq n_U \leq D$ is the number of distinct eigenvalues of U , and $k \in [1, d_\alpha]$, where d_α is the dimension of the subspace corresponding to the eigenvalue u_α . This decomposition can be extended to the operator space $\mathcal{B}(\mathcal{H})$, through

$$\mathcal{B}(\mathcal{H}) = \bigoplus_{\alpha=1}^{n_U} \bigoplus_{\beta=1}^{n_U} \mathcal{B}_{\alpha\beta}, \quad (6)$$

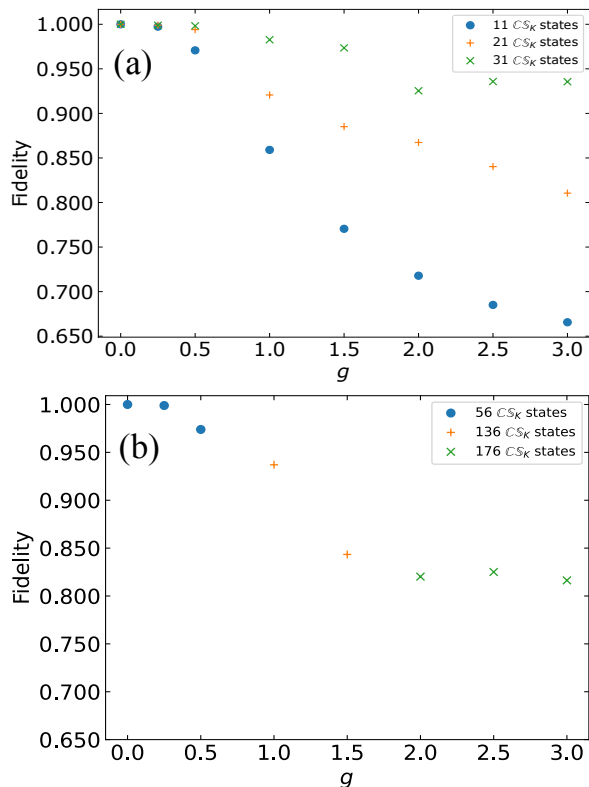


FIG. 2. Results for the transverse field Ising model with local dissipators described in the main text. The corresponding fidelity value between the state obtained and the theoretical state, for CS_K ansatz of different ansatz sizes K , are compared. **a)** Results for 5 qubits. **b)** Results for 8 qubits. For larger g , we note that the exact NESS becomes much less sparse. To continue to obtain good fidelities in this regime, we require larger number of states in our ansatz.

where $\mathcal{B}_{\alpha\beta} = \text{Span} \left\{ |\psi_\alpha^{(n)}\rangle \langle \psi_\beta^{(m)}| \right\}$, $n \in [1, d_\alpha]$, $m \in [1, d_\beta]$. Each orthogonal subspace can each contribute to the NESS solution, since each subspace $\mathcal{B}_{\alpha\beta}$ can have a solution $\rho_{\alpha\beta}$ such that $L[\rho_{\alpha\beta}] = 0$. Hence, our algorithm finds a solution which is a linear combination of the solutions from all the $\mathcal{B}_{\alpha\beta}$ subspaces. We note that physical density matrices (with unit trace) can only exist in the diagonal sub spaces $\mathcal{B}_{\alpha\alpha}$ due to the orthogonality between the eigenvectors from different \mathcal{H}_α . However, precisely because the unphysical density matrices from $\mathcal{B}_{\alpha\beta}$, $\alpha \neq \beta$ have trace 0, they can contribute to physical solutions found by forming linear combinations with a physical density matrix, which changes physical properties of the solution. There are at least n_U physical, distinct NESS, which we label as ρ_α^* , where $\rho_\alpha^* \in \mathcal{B}_{\alpha\alpha}$. If another strong symmetry is present, these n_U different ρ_α^* can be further decomposed into NESS from the new symmetry sectors.

Generalization of our method for multiple NESS.— We can systematically obtain all the physical steady

states that exist in all the symmetry subspaces for quantum systems with multiple steady states, if we have knowledge of the full Lindbladian. The simplest way would be to directly construct an ansatz that lies in the desired symmetry subspace. If we have the capacity on the quantum computer to generate such states, which has been demonstrated for Dicke states [55] and states that conserve total magnetization in the XXZ Heisenberg chain [56], we can simply generate such a set of states and use that to construct our hybrid ansatz for our algorithm. This method has the added advantage of reducing the size of the ansatz, due to the reduction of the possible solution space. For example, we use the quantum circuit proposed in [56] for the eight qubit XXZ Heisenberg chain with dephasing noise and obtained a fidelity of nearly 1 to the theoretical NESS in the $m = 4$ symmetry subspace with only 28 states in our ansatz. Here, m is the eigenvalue of the total magnetization operator M . However, this method is limited due to difficulty in devising circuits that conserve a general symmetry. Thus, we also propose two general methods to find multiple NESS.

The first method utilizes the SDP structure of the optimization. For each operator N_k that corresponds to the k th strong symmetry in our system, a NESS is found that is in the symmetry subspace corresponding to a particular eigenvalue n_k of N_k , by including the linear constraint $\text{Tr}(\beta \tilde{N}_k) = n_k$ in the SDP, where $(\tilde{N}_k)_{ij} = \langle \chi_i | N_k | \chi_j \rangle$. These additional linear constraints are additional, efficiently implementable, hyperplanes in the parameter space that the optimizer needs to fulfill.

As an example, we consider a XXZ Heisenberg chain on a system with n qubits, $H_{XXZ} = \sum_{j=1}^{n-1} \sigma_X^j \sigma_X^{j+1} + \sigma_Y^j \sigma_Y^{j+1} + \Delta \sigma_Z^j \sigma_Z^{j+1}$, and dephasing noise, defined by the n jump operators $L_i = \sigma_Z^i$. The total magnetization $M = \sum_{i=1}^n \sigma_Z^i$ commutes with the Hamiltonian and all jump operators L_i , generating a strong symmetry given by $S_z = e^{i\phi M}$. This gives rise to $n + 1$ magnetization blocks, each associated with an eigenvalue of M and has its own unique NESS.

Considering the additional constraint $\text{Tr}(\beta \tilde{M}) = m$, where $\tilde{M}_{ij} = \langle \chi_i | M | \chi_j \rangle$, our first method is able to obtain a solution which is in the m magnetization symmetry sector of M that agrees with the exact results. We emphasize that the usage of the quantum computer scales linearly with the number of constraints, as we do not need to measure the D, E, F, R matrices several times.

The second method does not require us to add additional constraints into the SDP, which allows our classical post processing to be more numerically stable. It utilizes the structure of a Vandermonde matrix to systematically remove the contributions from unwanted subspaces by applying the symmetry operator to the state and is discussed in detail in the Supplemental Information [45].

Conclusion.— We present a new algorithm for finding NESS solutions of open systems. Our approach re-

states the NESS problem as a feasibility SDP, which is a well known and well characterized optimization problem. We believe that this is the first work to apply this approach to solving master equations. As a consequence of our approach, we are able to utilize NISQ devices to aid a classical computer in its calculation, by offloading the difficult task of calculating expectation values of arbitrary Pauli strings to the quantum computer. Utilizing this quantum assisted approach to NISQ devices, our algorithm retains all of the advantages that such algorithms have over competitors that rely on variationally optimizing a quantum circuit.

Our algorithm provides three main advantages over its NISQ competitors. Firstly, since it frames the NESS problem as a feasibility SDP, it allows us to bypass many of the problems associated with traditional variational quantum algorithms on NISQ devices, such as the barren plateau problem and training over the non-convex landscape in the state space. Secondly, it provides a natural way to enforce the positivity constraint of density matrices during the optimization, along with any other constraints we would want to implement. One example where being able to enforce other constraints is when multiple steady states exist. Lastly, our method also gives us a systematic way to increase the expressibility of our ansatz without sacrificing trainability.

Our work opens up many avenues for research. NISQ devices are already utilized to study the ground states of chemical substances [57]. Most believe that studying open system many-body Hamiltonians, like the fermionic Hubbard model in the presence of generic dissipations, are classically intractable [58]. It is hoped NISQ devices and NISQ algorithms can make the simulation of such problems possible [59]. Our method extends these studies to open quantum systems and widens the range of applications. Furthermore, we believe our method can be used as a tool to assist environmental engineering [60] of open quantum systems. Studying how noise and ansatz choice affects quantum-assisted methods such as ours are interesting problems to consider in the future. We believe it is possible to extend our algorithm to allow constraints over continuous variables, which changes the optimization program into a semi-infinite feasibility problem [61]. We expect all of these to have a substantial impact on the NESS problem in the near and far term.

We are grateful to the National Research Foundation and the Ministry of Education, Singapore for financial support. SV acknowledges support from Government of India DST-SERB Early Career Research Award (ECR/2018/000957) and Government of India DST-QUEST grant number DST/ICPS/QuST/Theme-4/2019. K.B. acknowledges funding by the DoE ASCR Accelerated Research in Quantum Computing program (award No. DE-SC0020312), DoE QSA, NSF QLCI (award No. OMA-2120757), NSF PFCQC program, the DoE ASCR Quantum Testbed Pathfinder program

(award No. DE-SC0019040), U.S. Department of Energy Award No. DE-SC0019449, AFOSR, ARO MURI, AFOSR MURI, and DARPA SAVaNT ADVENT.

* Equal contribution

† sai@phy.iitb.ac.in

- [1] F. Schwarz, I. Weymann, J. von Delft, and A. Weichselbaum, *Phys. Rev. Lett.* **121**, 137702 (2018).
- [2] T. N. Ikeda and M. Sato, *Science advances* **6**, eabb4019 (2020).
- [3] S. Fraenkel and M. Goldstein, *SciPost Phys.* **11**, 85 (2021).
- [4] A. E. Raeber and D. A. Mazziotti, *Physical Chemistry Chemical Physics* **22**, 23998 (2020).
- [5] D. Manzano and P. Hurtado, *Advances in Physics* **67**, 1 (2018).
- [6] W. Foulkes, L. Mitas, R. Needs, and G. Rajagopal, *Reviews of Modern Physics* **73**, 33 (2001).
- [7] Z. Yan, L. Pollet, J. Lou, X. Wang, Y. Chen, and Z. Cai, *Phys. Rev. B.* **97**, 035148 (2018).
- [8] A. Nagy and V. Savona, *Phys. Rev. A.* **97**, 052129 (2018).
- [9] A. Nagy and V. Savona, *Phys. Rev. Lett.* **122**, 250501 (2019).
- [10] M. Zwolak and G. Vidal, *Phys. Rev. Lett.* **93**, 207205 (2004).
- [11] F. Verstraete, J. J. Garcia-Ripoll, and J. I. Cirac, *Phys. Rev. Lett.* **93**, 207204 (2004).
- [12] R. Orus and G. Vidal, *Phys. Rev. B.* **78**, 155117 (2008).
- [13] J. Cui, J. I. Cirac, and M. C. Bañuls, *Phys. Rev. Lett.* **114**, 220601 (2015).
- [14] A. H. Werner, D. Jaschke, P. Silvi, M. Kliesch, T. Calarco, J. Eisert, and S. Montangero, *Phys. Rev. Lett.* **116**, 237201 (2016).
- [15] A. A. Gangat, I. Te, and Y.-J. Kao, *Phys. Rev. Lett.* **119**, 010501 (2017).
- [16] A. Kshetrimayum, H. Weimer, and R. Orús, *Nat. Communications* **8**, 1 (2017).
- [17] F. Verstraete, V. Murg, and J. I. Cirac, *Advances in physics* **57**, 143 (2008).
- [18] H.-Y. Su and Y. Li, *Phys. Rev. A.* **101**, 012328 (2020).
- [19] Z. Hu, R. Xia, and S. Kais, *Scientific reports* **10**, 1 (2020).
- [20] A. W. Schlimgen, K. Head-Marsden, L. M. Sager, P. Narang, and D. A. Mazziotti, *Phys. Rev. Lett.* **127**, 270503 (2021).
- [21] Z. Liu, L.-M. Duan, and D.-L. Deng, *Phys. Rev. R.* **4**, 013097 (2022).
- [22] H. Kamakari, S.-N. Sun, M. Motta, and A. J. Minnich, *PRX Quantum* **3**, 010320 (2022).
- [23] N. Ramusat and V. Savona, *Quantum* **5**, 399 (2021).
- [24] N. Yoshioka, Y. O. Nakagawa, K. Mitarai, and K. Fujii, *Phys. Rev. R.* **2**, 043289 (2020).
- [25] E. Anschuetz, J. Olson, A. Aspuru-Guzik, and Y. Cao, in *International Workshop on Quantum Technology and Optimization Problems* (Springer, 2019) pp. 74–85.
- [26] X. You and X. Wu, in *International Conference on Machine Learning* (PMLR, 2021) pp. 12144–12155.
- [27] L. Bittel and M. Kliesch, *Phys. Rev. Lett.* **127**, 120502 (2021).
- [28] L. Vandenberghe and S. Boyd, *SIAM review* **38**, 49

- (1996).
- [29] S. Boyd and L. Vandenberghe, *Convex Optimization* (Cambridge University Press, 2004).
- [30] H. Wolkowicz, R. Saigal, and L. Vandenberghe, *Handbook of semidefinite programming: theory, algorithms, and applications*, Vol. 27 (Springer Science & Business Media, 2012).
- [31] H.-Y. Liu, T.-P. Sun, Y.-C. Wu, and G.-P. Guo, *Chinese Physics Letters* **38**, 080301 (2021).
- [32] M. Cerezo, A. Arrasmith, R. Babbush, S. C. Benjamin, S. Endo, K. Fujii, J. R. McClean, K. Mitarai, X. Yuan, L. Cincio, *et al.*, *Nat. Reviews Physics*, **1** (2021).
- [33] K. Bharti, A. Cervera-Lierta, T. H. Kyaw, T. Haug, S. Alperin-Lea, A. Anand, M. Degroote, H. Heimonen, J. S. Kottmann, T. Menke, *et al.*, *arXiv preprint arXiv:2101.08448*.
- [34] K. Bharti, T. Haug, V. Vedral, and L.-C. Kwek, *arXiv preprint arXiv:2106.03891*.
- [35] T. Haug and K. Bharti, *arXiv preprint arXiv:2011.14737*.
- [36] J. W. Z. Lau, T. Haug, L. C. Kwek, and K. Bharti, *arXiv preprint arXiv:2103.05500*.
- [37] K. H. Lim, T. Haug, L.-C. Kwek, and K. Bharti, *Quantum Science and Technology* (2021).
- [38] K. Bharti, *arXiv preprint arXiv:2009.11001*.
- [39] K. Bharti and T. Haug, *Phys. Rev. A*, **104**, L050401 (2021).
- [40] J. W. Z. Lau, K. Bharti, T. Haug, and L. C. Kwek, *arXiv preprint arXiv:2101.07677*.
- [41] C. Lanczos, *J. Res. Natl. Bur. Stand. B* **45**, 255 (1950).
- [42] W. E. Arnoldi, *Quarterly of applied mathematics* **9**, 17 (1951).
- [43] R. B. Lehoucq, D. C. Sorensen, and C. Yang, *ARPACK users' guide: solution of large-scale eigenvalue problems with implicitly restarted Arnoldi methods* (SIAM, 1998).
- [44] Y. Saad, *Numerical methods for large eigenvalue problems: revised edition* (SIAM, 2011).
- [45] See Supplemental Material at <https://journals.aps.org/prl/abstract/10.1103/PhysRevLett.130.240601> for (a) definition of cummulative \mathcal{K} moment states, (b) summary of the algorithm, (c) a comparison to alternative approaches, (d) a justification for ansatz and scaling arguments, (e) an algorithm to find multiple steady states. The Supplemental Material includes Refs. [46] and [47]
- [46] M. V. Ramana, *Mathematical Programming* **77**, 129 (1997).
- [47] B. Kalantari, *arXiv preprint arXiv:1911.03989*.
- [48] K. Mitarai and K. Fujii, *Phys. Rev. R.* **1**, 013006 (2019).
- [49] E. Knill, *arXiv preprint quant-ph/9508006*.
- [50] M. Möttönen, J. J. Vartiainen, V. Bergholm, and M. M. Salomaa, *Phys. Rev. Lett.* **93**, 130502 (2004).
- [51] J. J. Vartiainen, M. Möttönen, and M. M. Salomaa, *Phys. Rev. Lett.* **92**, 177902 (2004).
- [52] M. Plesch and Č. Brukner, *Phys. Rev. A*, **83**, 032302 (2011).
- [53] K. Seki and S. Yunoki, *PRX Quantum* **2**, 010333 (2021).
- [54] G.-V. Policharla and S. Vinjanampathy, *Phys. Rev. Lett.* **127**, 220504 (2021).
- [55] M. Vetrivelan and S. Vinjanampathy, *Quantum Science and Technology* **7**, 025012 (2022).
- [56] C. Lyu, X. Xu, M. Yung, and A. Bayat, *arXiv preprint arXiv:2203.02444* (2022).
- [57] Y. Nam, J.-S. Chen, N. C. Pienti, K. Wright, C. Delaney, D. Maslov, K. R. Brown, S. Allen, J. M. Amini, J. Apisdorf, *et al.*, *npj Quantum Information* **6**, 1 (2020).
- [58] N. Schuch and F. Verstraete, *Nature physics* **5**, 732 (2009).
- [59] O. Shtanko, A. Deshpande, P. S. Julienne, and A. V. Gorshkov, *PRX Quantum* **2**, 030350 (2021).
- [60] C. P. Koch, *Journal of Physics: Condensed Matter* **28**, 213001 (2016).
- [61] A. Ferrer, M. A. Goberna, E. González-Gutiérrez, and M. I. Todorov, *Annals of Operations Research* **258**, 587 (2017).
- [62] J. R. McClean, S. Boixo, V. N. Smelyanskiy, R. Babbush, and H. Neven, *Nat. Communications* **9**, 4812 (2018).
- [63] E. Grant, L. Wossnig, M. Ostaszewski, and M. Benedetti, *Quantum* **3**, 214 (2019).
- [64] M. Larocca, N. Ju, D. García-Martín, P. J. Coles, and M. Cerezo, *arXiv preprint arXiv:2109.11676*.
- [65] E. R. Anschuetz, *arXiv preprint arXiv:2109.06957*.
- [66] M. Kliesch, D. Gross, and J. Eisert, *Phys. Rev. Lett.* **113**, 160503 (2014).
- [67] A. Peruzzo, J. McClean, P. Shadbolt, M.-H. Yung, X.-Q. Zhou, P. J. Love, A. Aspuru-Guzik, and J. L. O'brien, *Nat. Communications* **5**, 4213 (2014).
- [68] A. Kandala, A. Mezzacapo, K. Temme, M. Takita, M. Brink, J. M. Chow, and J. M. Gambetta, *Nature* **549**, 242 (2017).
- [69] Y. Li and S. C. Benjamin, *Physical Review X* **7**, 021050 (2017).
- [70] X. Yuan, S. Endo, Q. Zhao, Y. Li, and S. C. Benjamin, *Quantum* **3**, 191 (2019).
- [71] M. Benedetti, M. Fiorentini, and M. Lubasch, *Phys. Rev. R.* **3**, 033083 (2021).
- [72] O. Higgott, D. Wang, and S. Brierley, *Quantum* **3**, 156 (2019).
- [73] G. Verdon, J. Marks, S. Nanda, S. Leichenauer, and J. Hidary, *arXiv preprint arXiv:1910.02071*.
- [74] C. Bravo-Prieto, D. García-Martín, and J. I. Latorre, *Phys. Rev. A*, **101**, 062310 (2020).
- [75] H.-Y. Huang, K. Bharti, and P. Rebentrost, *New Journal of Physics* **23**, 113021 (2021).
- [76] Z. Holmes, K. Sharma, M. Cerezo, and P. J. Coles, *arXiv preprint arXiv:2101.02138*.
- [77] D. J. Robinson, *Course In Linear Algebra With Applications, A* (World Scientific, 2006).
- [78] Boyd, S., El Ghaoui, L., Feron, E. & Balakrishnan, V. Linear matrix inequalities in system and control theory. (SIAM,1994)
- [79] Grant, M. & Boyd, S. CVX: Matlab software for disciplined convex programming, version 2.1. (2014)
- [80] Grant, M. & Boyd, S. Graph implementations for non-smooth convex programs. *Recent Advances In Learning And Control*. pp. 95-110 (2008)
- [81] Grant, M., Boyd, S. & Ye, Y. Disciplined convex programming. *Global Optimization*. pp. 155-210 (2006), https://web.stanford.edu/~boyd/papers/disc_cvx_prog.html
- [82] Brandao, F., Kueng, R. & França, D. Faster quantum and classical SDP approximations for quadratic binary optimization. *Quantum*. **6** pp. 625 (2022), <https://quantum-journal.org/papers/q-2022-01-20-625/>
- [83] Lin, Lin and Tong, Yu. Near-optimal ground state preparation. *Quantum*. **4** pp. 372 (2020), <https://quantum-journal.org/papers/q-2020-12-14-372/>

Appendix A: Definition of cumulative \mathcal{K} moment states

Given a Hamiltonian written as a linear combination of unitaries

$$\mathcal{H} = \sum_i^r \eta_i U_i, \quad (\text{A1})$$

we build an ansatz as a linear combination of quantum states

$$|\psi(\boldsymbol{\alpha})\rangle = \sum_i^L \alpha_i |\chi_i\rangle. \quad (\text{A2})$$

These quantum states $|\chi_i\rangle$ are chosen in a manner that utilizes the Krylov subspace of the original problem. With the form of the Hamiltonian above as well as a given state $|\psi\rangle$, we build the Krylov subspace up to order K , defined as

$$Kr_K \equiv \text{span} \{|\psi\rangle, H|\psi\rangle, \dots, H^K|\psi\rangle\} \quad (\text{A3})$$

We take each element of the subspace $H^k|\psi\rangle = (\sum_i \eta_i U_i)^k |\psi\rangle$ and multiply out the power k such that we get a sum. Each constituent term of this sum, which can be written as $U_{i_1} \dots U_{i_k} |\psi\rangle$, is then added to a set \mathbb{S}_k . Finally, we combine all $K+1$ sets \mathbb{S}_k into what we now call the fine-grained Krylov subspace basis or cumulative K -moment states $\mathbb{CS}_K \equiv \cup_{j=0}^K \mathbb{S}_j$, which is formally defined as follows [39].

Definition 1. Given a set of unitaries $\mathbb{U} \equiv \{U_i\}_{i=1}^r$, a positive integer K and some quantum state $|\psi\rangle$, K -moment states is the set of quantum states of the form $\{|\chi\rangle\}_K = \{U_{i_K} \dots U_{i_2} U_{i_1} |\psi\rangle\}_i$ for $U_{i_i} \in \mathbb{U}$. We denote the aforementioned set by \mathbb{S}_K . The fine-grained Krylov subspace basis or cumulative K -moment states \mathbb{CS}_K is defined as $\mathbb{CS}_K \equiv \cup_{j=0}^K \mathbb{S}_j$.

The success of such an ansatz for the NESS problem is highly dependent on the choice of the initial state $|\psi\rangle$ and also on the steady state being low rank. For the use case discussed here, it is generally hoped that the initial state has decent overlap with the steady state. If this is done, we expect that a sufficient ansatz can be generated for low k . It is known that the Hamiltonian ground state problem is QMA-hard and finding the steady state of a Liouvillian is probably of similar complexity. For most prior algorithms developed for NISQ computers for finding the ground state, they rely very heavily on utilizing ansatz that have some guarantee of overlap with the true ground state, of which without, it would not be feasible. Similarly, if we start out with a initial state that has exponentially small overlap with the true steady state, this method of generating an ansatz will not be efficient.

A variant of the \mathbb{CS}_K ansatz that we use in the main text for the five and eight qubit transverse field Ising model is to define $\mathbb{CS}_K \equiv \cup_{j=0}^K \mathbb{S}'_j$ where \mathbb{S}'_1 is a random subset with cardinality q of \mathbb{S}_1 , and \mathbb{S}'_j is defined as a random subset with cardinality q of the set $\{U_i |\phi\rangle | U_i \in \mathbb{U} \text{ and } |\phi\rangle \in \mathbb{S}_{j-1}\}$. This variant of the \mathbb{CS}_K ansatz has a smaller cardinality than the \mathbb{CS}_K ansatz defined above, at a cost of lower expressibility. For this particular variant of the \mathbb{CS}_K ansatz, it is more meaningful to quantify the expressibility of \mathbb{CS}_K by using the number of ansatz states in each \mathbb{CS}_K rather than using the index K itself.

Appendix B: Description of feasibility SDP

The typical Semidefinite programming (SDP) problem is one that minimizes a linear function of a cost function subject to the positive semi-definite condition and additional m constraints

$$\min_{\beta} \text{Tr}(A\beta), \quad (\text{B1})$$

$$\text{subject to } \beta \succcurlyeq 0, \quad (\text{B2})$$

$$\text{Tr}(C_i\beta) = c_i, i = 1, \dots, m. \quad (\text{B3})$$

We note that although the standard form for these additional m constraints is to be expressed as a trace constraint, this is not necessary. The works of Boyd, along with [30], offer alternate forms of SDPs that are not formulated with trace constraints.

In this paper, instead of formulating the problem as a typical SDP, it is formulated as a feasibility SDP problem [29]. In this problem, the cost function is removed. The program now attempts to find if it is possible to find a β subject to the positive semi-definite condition and the additional m trace constraints. Once the algorithm finds a β , the program stops and reports the solution. There is hence no concept of a cost function to be minimized. The exact complexity of this problem is still unknown, though it is highly suspected that the feasibility SDP is polynomial in the size of the matrix [46]. Furthermore, it has been shown that certain classes of feasibility SDPs still can be efficiently solved [47].

The feasibility SDP problem can be solved with existing SDP solvers, by setting the cost function to 0. As mentioned in the main manuscript, we rely on CVX to solve the SDPs in this work.

Appendix C: Summary of the algorithm

We can summarise our algorithm as a three step procedure, namely

1. Write the ansatz $\rho = \sum_{i,j} \beta_{ij} |\chi_i\rangle \langle \chi_j|$, where $|\chi_i\rangle \in \mathbb{C}\mathbb{S}_K$. With this ansatz, the Linblad master equation is given by

$$-i(D\beta E - E\beta D) + \sum_n \gamma_n \left(R_n \beta R_n^\dagger - \frac{1}{2} F_n \beta E - \frac{1}{2} E \beta F_n \right) = 0. \quad (\text{C1})$$

where the matrices D, E, R_n, F_n have matrix elements $E_{ij} = \langle \chi_i | \chi_j \rangle$, $D_{ij} = \langle \chi_i | H | \chi_j \rangle$, $R_{(n),ij} = \langle \chi_i | A_n | \chi_j \rangle$ and $F_{(n),ij} = \langle \chi_i | A_n | \chi_j \rangle$

2. Measure the matrix elements of the D, E, R_n, F_n matrices on a quantum computer.
3. Solve the following feasibility SDP on a classical computer, written as

$$\text{Find } \beta \text{ s.t. } -i(D\beta E - E\beta D) + \sum_n \gamma_n \left(R_n \beta R_n^\dagger - \frac{1}{2} F_n \beta E - \frac{1}{2} E \beta F_n \right) = 0, \quad (\text{C2a})$$

$$\beta \succcurlyeq 0, \quad (\text{C2b})$$

$$\text{Tr}(\beta E) = 1. \quad (\text{C2c})$$

Appendix D: Extra results for 5 qubits

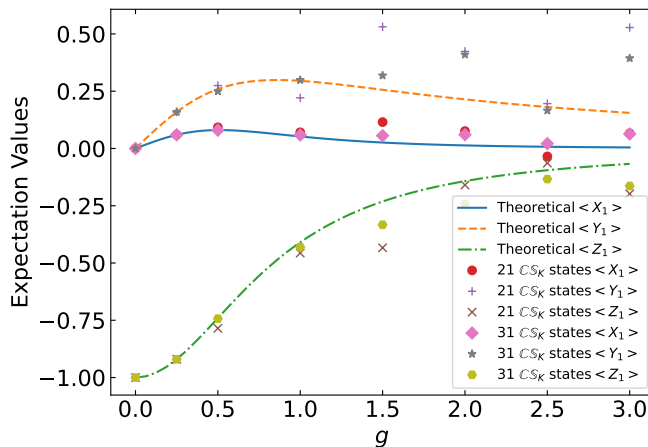


FIG. 3. Presented here are extra results for the 5-qubit model to supplement the results in the main manuscript. Shown are the expectation values of various observables for the steady states we obtained for the five qubit transverse field Ising model ($\gamma = 1$).

Appendix E: Overlap of initial state used to generate \mathbb{CS}_K states for 8 qubits

The effectiveness of the \mathbb{CS}_K method to generate basis states for the ansatz relies heavily on choosing an initial state with a non-exponentially decreasing overlap with the exact NESS. In general, we believe this is hard, due to the fact that it is probably closely related to the ground state problem, which is QMA-hard. In our simulations for 8 qubits, we rely on using a starting state that is an eigenstate with the largest eigenvalue of the exact NESS. In Table I we show the overlap of such a state with the exact NESS. Even with such a method, for large g , this is not very effective in producing a good steady state. We attribute the need for larger ansatz sizes in the large g case to this reason.

	$g = 0$	$g = 0.25$	$g = 0.5$	$g = 1$	$g = 1.5$	$g = 2$	$g = 2.5$	$g = 3$
Overlap	1	0.811	0.469	0.123	0.0474	0.0263	0.0181	0.0141

TABLE I. Comparison of the fidelity of the starting states with the exact NESS solution that were used to construct the \mathbb{CS}_K ansatz for the 8 qubit example discussed in the main manuscript. As g increases, we see that it is harder to find good starting states with non-vanishing overlap with the actual NESS.

Appendix F: Extra results for 8 qubits and detailed comparison with existing approach

Here, we present extra results for the 8 qubit transverse field Ising model for easy comparison to the currently existing Variational Quantum Algorithm (VQA)-based approach in [24]. This is shown in Fig. 4. We also perform a detailed resource comparison of both our approach and the VQA-based approach in [24] based on what was mentioned in Appendix G.

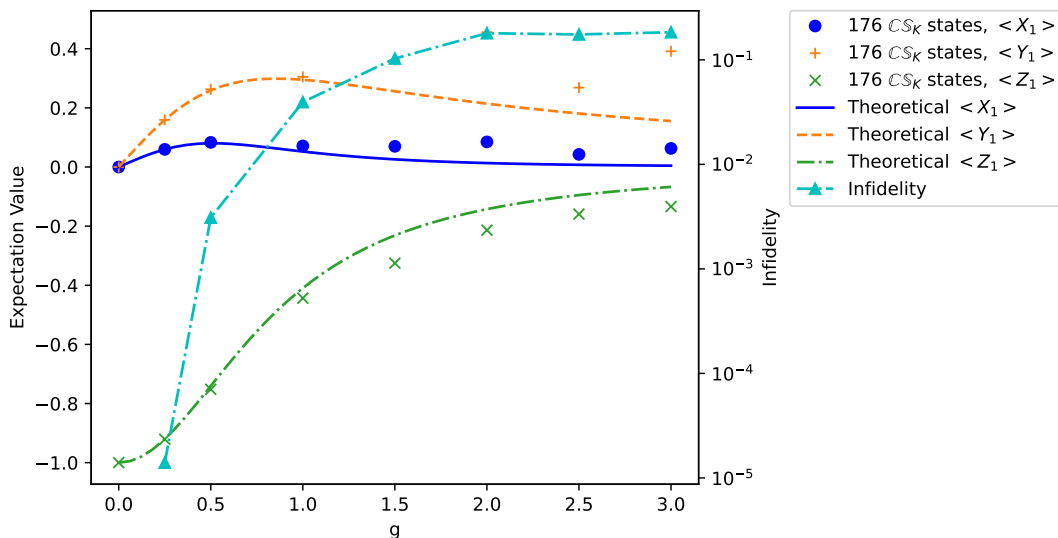


FIG. 4. Presented here are extra results for the 8-qubit model to supplement the results in the main manuscript. Shown are the expectation values of various observables for the steady states we obtained for the eight qubit transverse field Ising model ($\gamma = 1$). The ansatz size used in this simulation was a \mathbb{CS}_K ansatz comprising of 176 constituent states.

First, we list down the resource requirements of the VQA-based approach in [24]. Each evaluation of the cost function $\langle \rho(\vec{\theta}) | \mathcal{L}^\dagger \mathcal{L} | \rho(\vec{\theta}) \rangle$ in their VQA requires the evaluation of 1713 16-qubit quantum circuits. Assuming that their classical-quantum feedback loop requires N evaluations of the cost function, this means that they need to evaluate at least $1713 \times N$ 16-qubit quantum circuits. N is in general a large number, since the classical VQA optimisation is shown to be NP-hard [27] and also due to the well-known issue with barren plateaus that VQAs face.

On the other hand, for our SDP based method, we need to evaluate the matrix elements E_{ij} , D_{ij} , and R_{ij} , F_{ij} for both the phase-damping and amplitude damping dissipators. Assuming that we have M states in our ansatz, this means that in the worst case we need to measure $20 \times (M^2 + M) - M$ 8-qubit quantum circuits. Usually, we need

less measurements than that because there would be matrix elements that are repeated, based on the ansatz that we chose. Recall that once we have measured the matrix elements on the quantum computer, we don't need the quantum computer anymore. What remains is the classical SDP optimisation which is convex and hence classically tractable. As can be seen in Fig. 4, for small values of g , we can get good fidelity with $M = 176$, which means that we need to evaluate about 622864 8-qubit quantum circuits.

Based on the above analysis, as long as the VQA method requires more than $N \approx 360$ evaluations of the cost function, our SDP method (in the worst case) outperforms the VQA method in terms of number of measurements required. Furthermore, to reiterate, our method requires the measurement of 8-qubit quantum circuits, whereas the VQA method in [24] requires the measurement of 16-qubit quantum circuits. We can give a lower bound on the number of cost function evaluations in the VQA approach with the following argument. In the minimization of the cost function with gradient descent with the VQA approach, assuming a fixed step size, we need $O(\frac{1}{\epsilon})$ number of steps at least for the cost function to be accurate up to ϵ . Hence, assuming we set $\epsilon = 0.01$, we need at least 100 steps in the gradient descent. With 47 parameters in the quantum circuit in [24], each step of the gradient descent algorithm requires at least 47 evaluations of the cost function, since the computation of the gradient at each step requires us to independently vary each parameter at least once. Thus, at least 47 evaluations of the cost function at each step for at least 100 steps means that the VQA approach requires at least $N = 4700$ evaluations of the cost function to achieve an accuracy up to $\epsilon = 0.01$. This lower bound already exceeds $N = 360$, which means that the lower bound of the amount of quantum resources required to get the cost function to be accurate up to 0.01 already exceeds the amount of quantum resources required on our end. We note that the argument to derive this lower bound does not take into account the NP-hardness of the VQA optimisation and the issue with Barren Plateaus, both of which would increase N significantly. In our own numerical experiments of the VQA method using the classical BFGS optimiser, we did not achieve convergence even after $N = 900$. This means that when we compare both methods, our method requires a lot lesser measurements of 8-qubit quantum circuits in the worst case than the amount of measurements on 16-qubit quantum circuits required by [24] in the best case.

Appendix G: Comparison to alternative approaches

VQAs have been investigated in detail, and some of the drawbacks of using VQAs include the existence of barren plateaus [62, 63], the classical quantum feedback loop being a major bottleneck on current cloud-based quantum computers, and finally the fact that the classical optimisation program does not belong to any class of mathematically well-studied programs. Furthermore, recent work has shown that VQAs a large number of parameters to be useful [64, 65]. Some VQAs also require complicated multi-qubit controlled unitaries. Hence, the application of VQAs to study NESS in [24] inherits all of these aforementioned drawbacks. Furthermore, the work in [24] requires n ancilla qubits to solve an n qubit problem due to their approach of mapping an n qubit density matrix to a $2n$ qubit statevector. Lastly, it is unclear how the positivity of the density matrix is maintained over the course of the variational optimisation. This problem is possibly a difficult one, since it is known that checking the positivity of a density matrix in tensor network methods is NP-hard [66].

The canonical example of a VQA is the variational quantum eigensolver (VQE) [67, 68], which aims to solve for the ground state of a given Hamiltonian. Other examples of areas where VQAs have found application include quantum simulation [69–71], finding of excited states [72], quantum thermalization [73], numerical solvers [25, 74, 75], to name a few.

As shown in our Table II, our algorithm addresses some of the challenges in VQA/VQE based methods such as in [24].

We would also like to mention that for VQA based methods, the problem of how to systematically obtain an ansatz for such algorithms that is expressible enough to approximate the solution to a desired accuracy, yet retain trainability, is inherent and might be insurmountable. It has been shown that to get an expressible enough ansatz in such a framework, demands a fundamental tradeoff with the trainability of such an ansatz [76].

Appendix H: Justification for ansatz, and scaling arguments

The scaling of our algorithm is fundamentally related to the problem of obtaining an appropriate ansatz that is expressible enough. It is known that to prepare an arbitrary state on an n qubit quantum computer, we require a circuit depth of at least $2^n/n$ [49–52]. This is a complexity theoretic statement that cannot be bypassed by any quantum simulation algorithm based on parametric quantum circuits or linear combination of quantum states, and

TABLE II. Comparison of our solution to NESS problem to other solutions.

	VQE based methods [24]	Our algorithm
Ansatz	Parameterized quantum state ansatz.	Hybrid density matrix ansatz.
Variational parameters	Utilizes a parameterized quantum state/circuit. Variational parameters modify the quantum state on the quantum computer.	Utilizes a classical combination of quantum states. Variational parameters are the coefficients defining the linear superposition of the quantum states of the ansatz, do not modify the quantum state on the quantum computer.
Feedback loop	Requires a classical-quantum feedback loop, constantly modifying quantum state on the quantum computer.	Once measurements are made on quantum computer, no longer require usage of quantum computer, no need for classical-quantum feedback loop.
Training landscape	Non-convex landscape, optimization shown to be NP-hard, have exponentially many local minima far away from global minima.	Convex landscape.
Ansatz selection	Usually rely on problem agnostic ansatz such as Hardware Efficient ansatz, no guarantee of systematic improvement.	Problem aware ansatz. Systematic way to improve without sacrificing trainability.
Optimization program	Generally does not belong in any mathematically well studied class of programs.	Feasibility SDP, mathematically well characterized and studied.
Positivity constraint	Not aware of how to systematically enforce positivity constraint for density matrix.	Systematic way to enforce, built into optimization program.
Multiple NESS solutions	Not clear how to find multiple solutions in the presence of strong symmetries.	Systematic ways to find multiple solutions exist, such as adding linear constraints into the SDP optimisation.

indicates that our algorithm shares the worst case of requiring an exponentially large ansatz to obtain perfect fidelity with other variational algorithms, in the case of a general Hamiltonian with no symmetries and which is ergodic.

Thus, a large contributing factor to how our algorithm will scale hinges on the manner which we choose the $|\chi_i\rangle$ states which we generate our hybrid density matrix ansatz with. As such, a justification for the manner which we generate those states will be provided in this appendix (first given in [39]), before we discuss the scaling of our algorithm. Our justification relies on similar ideas to the method of using imaginary time evolution to find the ground state on classical computers. Suppose the initial state (0-moment state) $|\psi\rangle$ can be expressed in the eigenbasis of the Hamiltonian H ,

$$|\psi\rangle = \sum_{i=1}^{\mathcal{N}} a_i |\phi_i\rangle, \quad (\text{H1})$$

where $a_i \in \mathbb{C}$ for $i \in \{1, 2, \dots, \mathcal{N}\}$. Now we consider the normalized state if we apply the operator $\exp(-\tau H)$ for some $\tau \geq 0$ on the initial state:

$$|\gamma\rangle = \frac{e^{-\tau H} |\psi\rangle}{\sqrt{\langle \psi | e^{-2\tau H} | \psi \rangle}}. \quad (\text{H2})$$

In normal imaginary time evolution, this is the point where we recognize that if $\tau \rightarrow \infty$, $|\gamma\rangle \rightarrow |E_0\rangle$, where $|E_0\rangle$ is

the ground state. We consider the power series expansion $e^{-\tau H} = \sum_{p=0}^{\infty} \frac{(-\tau H)^p}{p!}$,

$$|\gamma\rangle = \frac{\sum_{p=0}^{\infty} \frac{(-\tau H)^p}{p!} |\psi\rangle}{\sqrt{\langle\psi| \sum_{p=0}^{\infty} \frac{(-2\tau H)^p}{p!} |\psi\rangle}}. \quad (\text{H3})$$

Let us also define the operator

$$\mathcal{O}^K \equiv \sum_{p=0}^K \frac{(-\tau H)^p}{p!}, \quad (\text{H4})$$

for $K \geq 0$. We note that \mathcal{O}^K corresponds to the sum of first K terms of $e^{-\tau H}$, or in other words a sum of elements of the Krylov subspace of H and $|\psi\rangle$ up to K , where the Krylov subspace is defined as per Eq. (A3). Using \mathcal{O}^K , we proceed to define

$$|\gamma_K\rangle \equiv \frac{\sum_{p=0}^K \frac{(-\tau H)^p}{p!} |\psi\rangle}{\sqrt{\langle\psi| \left(\sum_{p=0}^K \frac{(-\tau H)^p}{p!}\right)^2 |\psi\rangle}}. \quad (\text{H5})$$

For $K \rightarrow \infty$, $|\gamma_K\rangle \rightarrow |\gamma\rangle$. Remembering that we are expressing the Hamiltonian as a linear combination of unitaries, it is easy to see that $|\gamma_K\rangle$ can be written as linear combination of cumulative K -moment states, i.e.,

$$|\gamma_K\rangle = \sum_{|\chi_i\rangle \in \text{CS}_K} \alpha_i |\chi_i\rangle$$

where the combination coefficients $\alpha_i \in \mathbb{C}$. The aforementioned arguments justify our choice of ansatz as a linear combination of cumulative K -moment states.

In the worst case, the number of overlaps scales as $O(r^K)$ for r terms in H . This is fundamentally an expressibility problem, present in all NISQ variational algorithms, be it based on linear combination of states or those based on parametric quantum circuits. It is known that to prepare an arbitrary state on an n qubit quantum computer, we require a circuit depth of at least $2^n/n$ [49–52]. This suggests that it is very hard to produce an expressible enough ansatz to reproduce an arbitrary quantum state in the Hilbert space.

Appendix I: An algorithm to find multiple steady states

Before we proceed, we make the assumption that our symmetry operator U can be written as a linear combination of r tensored-Pauli operators P_i , namely

$$U = \sum_{i=0}^r \gamma_i P_i, \quad \gamma_i \in \mathbb{C}. \quad (\text{I1})$$

Under this assumption, it is easily to calculate powers of U , i.e U^k can be expanded in the same Pauli basis as $U^k = \sum_{i=0}^{r'} \gamma'_i P_i$. Hence, given a ρ of the form used in the paper, we have

$$\begin{aligned} \text{Tr}(\rho U^k) &= \sum_{m=0}^{r'} \gamma'_m \sum_{ij} \beta_{ij} \langle \chi_i | P_m | \chi_j \rangle \\ &= \sum_{m=0}^{r'} \gamma'_m \text{Tr}(\beta Q_m). \end{aligned} \quad (\text{I2})$$

where Q_m is the matrix with matrix elements $\langle \chi_i | P_m | \chi_j \rangle$. Now, we can efficiently calculate the matrix elements $\langle \chi_i | P_m | \chi_j \rangle$ on the quantum computer since $|\chi_i\rangle \in \text{CS}_K$ [38, 39]. Hence, we see that once we have the β that corresponds to ρ , we can easily compute terms like $\text{Tr}(\rho U^k)$ on the quantum computer by measuring $\langle \chi_i | P_m | \chi_j \rangle$ on the quantum computer. The above argument can be similarly extended to show that for an observable O written as a linear

combination of tensored-Pauli operators, we can easily compute terms like $\text{Tr}(\rho O U^k)$, $\text{Tr}(U^k \rho O)$, $\text{Tr}(U^k \rho U^{k'} O)$ on the quantum computer once we have β_{ij} .

We illustrate the main idea here with a simple, pedagogical example. Assume there exists a symmetry operator U with eigenvalues ± 1 . This gives rise to 4 symmetry sectors in \mathcal{B} , $\mathcal{B}_{++}, \mathcal{B}_{+-}, \mathcal{B}_{-+}, \mathcal{B}_{--}$ with corresponding density matrices $\rho_{++}, \rho_{+-}, \rho_{-+}, \rho_{--}$ such that $L[\rho_{\alpha,\beta}] = 0$, $\alpha, \beta = +, -$. Here, ρ_{++} and ρ_{--} correspond to physical density matrices and are the two NESS, while ρ_{+-} and ρ_{-+} are traceless and unphysical. We first obtain a single solution ρ by solving the SDP. This solution is a linear combination, $\rho = a\rho_{++} + b\rho_{+-} + c\rho_{-+} + d\rho_{--}$. We note that $\rho' = U\rho U^\dagger = a\rho_{++} - b\rho_{+-} - c\rho_{-+} + d\rho_{--}$, which implies $\rho'' = \frac{1}{2}(\rho + \rho') = a\rho_{++} + d\rho_{--}$. We thus obtain ρ_{++} (ρ_{--}) by evaluating $(\rho'' + (-)U\rho'')/2$.

As an example, we drive the aforementioned n qubit H_{XXZ} with two non-local Lindblad jump operators, namely $A_{XXZ}^1 = \sqrt{\Gamma(1-\mu)}\sigma_+^1\sigma_-^n$ and $A_{XXZ}^2 = \sqrt{\Gamma(1+\mu)}\sigma_-^1\sigma_+^n$, where $\sigma_\pm^j = (\sigma_X^j \pm i\sigma_Y^j)/2$, $\Gamma > 0$ and $\mu \in [0, 1]$ [5]. There are two unitary symmetry operators, $S_z = e^{i\phi M}$ and $S \equiv P \prod_{j=1}^n \sigma_X^j$, where P is the operator that exchanges site j with site $L - j + 1$ for all j . This can be defined using the computational basis. If the eigenvectors of σ_Z^j are expressed as $|s_1, \dots, s_n\rangle$, where $s_j \in \{0, 1\}$, P is defined as $P \equiv \sum_{(s_1, \dots, s_n) \in \{0, 1\}^n} |s_1, \dots, s_n\rangle \langle s_n, \dots, s_1|$. We can show that $[S, H_{XXZ}] = [S, A_{XXZ}^1] = [S, A_{XXZ}^2] = 0$, and also that S has two eigenvalues (± 1). Thus we would expect four different invariant subspaces, of which only two hold physical steady states, and the other two subspaces can contribute as components of a physical solution. We start with a solution obtained from method one that is in a selected symmetry subsection of M , that has contributions from all the steady state solutions of S . The second method can next be applied to remove the contributions from unwanted symmetry sectors of S . Our approach was tested up to system sizes of eight qubits, to find two trace orthogonal solutions ($\text{Tr}(\rho_1^\dagger \rho_2) = 0$) in the zero magnetization symmetry sector of M , which each solution corresponding to a physical steady state of the symmetry operator S . Our algorithm gave results that were in agreement with the exact results.

Now to describe the method in more detail, denoting ρ_α^* as the physical NESS belonging to a particular symmetry subspace, the goal is then to obtain all of the ρ_α^* , which is equivalent to finding all of the corresponding β_α^* , since once we do so, we can compute expectation values of the form $\text{Tr}(O\rho_\alpha^*)$. For simplicity, we shall assume below that there is only 1 strong symmetry (only one symmetry operator U), though the method detailed below easily generalises for multiple symmetries. Without loss of generality, let the operator U have n_U distinct eigenvalues which we know and label as $e^{i\lambda_1}, \dots, e^{i\lambda_{n_U}}$. As mentioned in the main text, running our algorithm once gives us a $\rho^{(1)}$ that is the following linear combination:

$$\rho^{(1)} = \sum_{\alpha, \beta} c_{\alpha, \beta}^{(1)} \rho_{\alpha, \beta}, \quad \rho_{\alpha, \beta} \in \mathcal{B}_{\alpha, \beta} \quad (13)$$

where the coefficients $c_{\alpha, \beta}^{(1)}$ are unknown to us. Here, $\rho_{\alpha, \beta}$ are the density matrices such that $L[\rho_{\alpha, \beta}] = 0$. The general method is to first systematically eliminate the contributions from the subspaces $\mathcal{B}_{\alpha, \beta}$, $\alpha \neq \beta$ in the above linear combination. To do so, we note that

$$U\rho^{(1)}U^\dagger = \sum_{\alpha} c_{\alpha, \alpha}^{(1)} \rho_{\alpha, \alpha} + \sum_{\alpha \neq \beta} e^{i(\lambda_\alpha - \lambda_\beta)} c_{\alpha, \beta}^{(1)} \rho_{\alpha, \beta} \quad (14)$$

which means that

$$\rho^{(1)} - U\rho^{(1)}U^\dagger = \sum_{\alpha \neq \beta} \left(1 - e^{i(\lambda_\alpha - \lambda_\beta)}\right) c_{\alpha, \beta}^{(1)} \rho_{\alpha, \beta} \quad (15)$$

Now, to eliminate the contribution from the $\mathcal{B}_{m, n}$, $m \neq n$ subspace, we define $\rho^{(2)}$ as follows:

$$\rho^{(2)} = \rho^{(1)} - \frac{(\rho^{(1)} - U\rho^{(1)}U^\dagger)}{1 - e^{i(\lambda_m - \lambda_n)}} = \sum_{\substack{\alpha, \beta \\ \alpha \neq m \\ \beta \neq n}} c_{\alpha, \beta}^{(2)} \rho_{\alpha, \beta} \quad (16)$$

where

$$c_{\alpha, \beta}^{(2)} = \begin{cases} c_{\alpha, \alpha}^{(1)} & \text{if } \alpha = \beta \\ \left(1 - \frac{1 - e^{i(\lambda_\alpha - \lambda_\beta)}}{1 - e^{i(\lambda_m - \lambda_n)}}\right) c_{\alpha, \beta}^{(1)} & \text{if } \alpha \neq \beta \end{cases} \quad (17)$$

We see that even though we do not know the coefficients in the linear combinations in Eq. (I3), we can systematically eliminate the contribution from $\mathcal{B}_{m,n}$ by considering linear combinations of the terms $\rho^{(1)}$ and $U\rho^{(1)}U^\dagger$. Now, since Eq. (I6) is of the same form as Eq. (I3), but just without the contribution from the subspace $\mathcal{B}_{m,n}$, we can pick another subspace $\mathcal{B}_{o,p}$ with $o \neq p$ and follow the same process to get a density matrix $\rho^{(3)}$ but with the contribution from $\mathcal{B}_{o,p}$ eliminated. It is easy to see that we can continue this process until we have a density matrix ρ^{phys} which only contains linear combinations of physical density matrices, i.e

$$\rho^{\text{phys}} = \sum_{\alpha=1}^{n_U} c_\alpha \rho_{\alpha,\alpha} \quad (\text{I8})$$

Note that at this stage, we have ρ^{phys} written as a linear combination of terms $\rho^{(1)}$, $U\rho^{(1)}U^\dagger$, $U^2\rho^{(1)}(U^\dagger)^2$, etc, where $\rho^{(1)}$ is the solution that our algorithm originally gave us. Now, with Eq. (I8), we can obtain $c_\alpha \rho_{\alpha,\alpha}$ as a linear combination of the matrices ρ^{phys} , $U\rho^{\text{phys}}$, \dots , $U^{n_U-1}\rho^{\text{phys}}$. To see this, we note that we have

$$\begin{pmatrix} U^0 \rho^{\text{phys}} \\ U^1 \rho^{\text{phys}} \\ \vdots \\ U^{n_U-1} \rho^{\text{phys}} \end{pmatrix} = V \begin{pmatrix} c_1 \rho_{11} \\ c_2 \rho_{22} \\ \vdots \\ c_{n_U} \rho_{22} \end{pmatrix} \quad (\text{I9})$$

where

$$V = \begin{pmatrix} 1 & 1 & \dots & 1 \\ e^{i\lambda_1} & e^{i\lambda_2} & \dots & e^{i\lambda_{n_U}} \\ \vdots & \vdots & \vdots & \vdots \\ e^{i(n_U-1)\lambda_1} & e^{i(n_U-1)\lambda_2} & \dots & e^{i(n_U-1)\lambda_n} \end{pmatrix} \quad (\text{I10})$$

is the Vandermonde matrix [77]. Since $e^{i\lambda_\alpha}$ are the n_U distinct eigenvalues of U , the Vandermonde matrix is invertible. Once we have $c_\alpha \rho_{\alpha,\alpha}$, we can just normalise it by its trace to give us a density matrix $\rho_{\alpha,\alpha} \in \mathcal{B}_{\alpha,\alpha}$ such that $L[\rho_{\alpha,\alpha}] = 0$. Note that at this stage, we have $\rho_{\alpha,\alpha}$ as a linear combination of terms like $U^k \rho^{(1)} U^{k'}$ for some $k, k' \in \mathbb{Z}^+$, where $\rho^{(1)}$ is the solution that our SDP algorithm gave. For an observable O written as a linear combination of tensored-Pauli operators, we can easily obtain $\text{Tr}(\rho_{\alpha,\alpha} O)$ in a similar fashion as in Eq. (I2) by using the fact that O and U are both linear combination of tensored-Pauli operators, and hence in the end, we only need to evaluate terms like $\langle \chi_i | P | \chi_j \rangle$ on the quantum computer, where P is a tensored-Pauli operator. We note that the method described above to get ρ_α^* works only if the coefficient $c_{\alpha,\alpha}^{(1)}$ in $\rho^{(1)}$ is not zero. Since $\rho^{(1)}$ is obtained from an SDP feasibility program, if we encounter the aforementioned scenario where $c_{\alpha,\alpha}^{(1)} = 0$, we can possibly re-run the feasibility program with a different starting guess and get a different $\rho^{(1)}$. From our numerical simulations, there is good evidence to suggest that this situation is exceedingly rare.